
Training-free Editioning of Text-to-Image Models

Jinqi Wang
Cardiff University
WangJ159@cardiff.ac.uk

Yunfei Fu
iArt.ai
yunfei@iart.ai

Zhangcan Ding
iArt.ai
zhangcan@iart.ai

Bailin Deng
Cardiff University
DengB3@cardiff.ac.uk

Yu-Kun Lai
Cardiff University
LaiY4@cardiff.ac.uk

Yipeng Qin*
Cardiff University
QinY16@cardiff.ac.uk

Abstract

Inspired by the software industry’s practice of offering different editions or versions of a product tailored to specific user groups or use cases, we propose a novel task, namely, *training-free editioning*, for text-to-image models. Specifically, we aim to create variations of a base text-to-image model without retraining, enabling the model to cater to the diverse needs of different user groups or to offer distinct features and functionalities. To achieve this, we propose that different editions of a given text-to-image model can be formulated as *concept subspaces* in the latent space of its text encoder (e.g., CLIP). In such a concept subspace, all points satisfy a specific user need (e.g., generating images of a cat lying on the grass/ground/falling leaves). Technically, we apply Principal Component Analysis (PCA) to obtain the desired concept subspaces from representative text embedding that correspond to a specific user need or requirement. Projecting the text embedding of a given prompt into these low-dimensional subspaces enables efficient model editioning without retraining. Intuitively, our proposed editioning paradigm enables a service provider to customize the base model into its “cat edition” (or other editions) that restricts image generation to cats, regardless of the user’s prompt (e.g., dogs, people, etc.). This introduces a new dimension for product differentiation, targeted functionality, and pricing strategies, unlocking novel business models for text-to-image generators. Extensive experimental results demonstrate the validity of our approach and its potential to enable a wide range of customized text-to-image model editions across various domains and applications.

1 Introduction

Recent advances in text-to-image models [40, 27, 25, 28, 23, 1, 8] have revolutionized visual content creation, enabling users to create highly realistic images from natural language descriptions. However, as these models become more widely adopted, service providers face challenges in monetizing them and tailoring offerings to diverse customer needs. In the software industry, providers overcome this by offering product editions or versions tailored to specific user segments, e.g., Home Edition, Professional Edition, Enterprise Edition. In this work, we propose a novel task, namely, *training-free editioning*, and applies this strategy to text-to-image models.

Our core idea is creating model variations without retraining to cater to differing customer needs or offer distinct features, formulating editions as *concept subspaces* within the embedding space of the model’s text encoder. Our concept subspace encapsulates points satisfying a user requirement (i.e., concept), e.g., cat images with specific choices of backgrounds. Technically, we apply Principal

*Corresponding author: Yipeng Qin

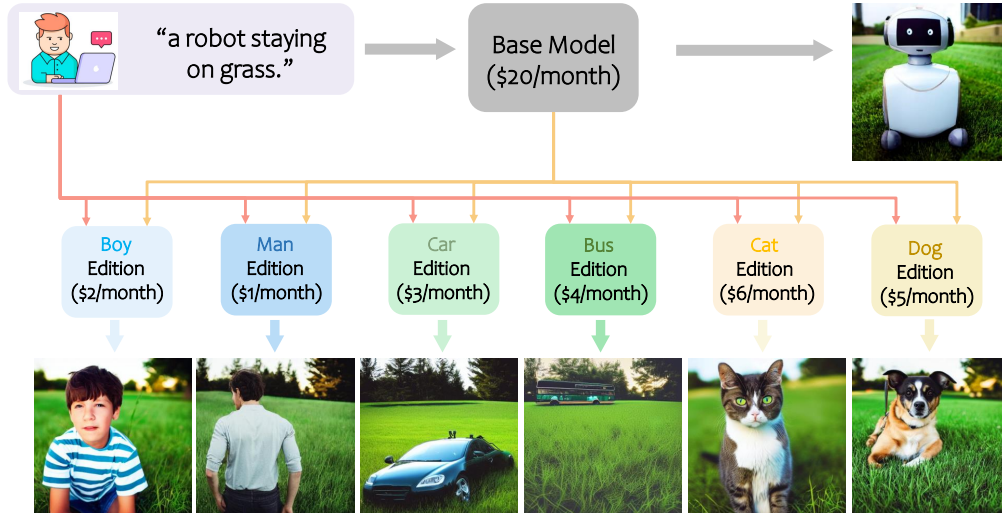


Figure 1: Illustration of **Text-to-Image Model Editioning**. Our method can create variations (e.g., *Boy Edition*, *Cat Edition*) of a *base* text-to-image model without retraining, enabling them to cater to the diverse needs of different user groups or to offer distinct features and functionalities.

Component Analysis (PCA) to text embeddings corresponding to a given concept and retain principal components capturing key variations to obtain a low-dimensional subspace for that concept within the original embedding space. Then, we achieve training-free editioning of text-to-image models by projecting the embeddings of input prompts into these subspaces.

Crucially, our approach allows service providers to efficiently customize the base model into targeted “editions” satisfying diverse customer needs without costly retraining. This leverages the pre-trained model’s capabilities while enabling fine-grained control over outputs. Providers can create tailored editions for different verticals, user types, or functionality tiers - e.g. a “cat edition” restricting outputs to cat images regardless of the input prompt (e.g., dogs, people). This unlocks innovative product strategies like freemium models with basic free editions versus feature-rich premium paid editions, enforcing content filters, specialty domains, or custom functionality per edition. Rather than offering an open-ended general tool, our paradigm shifts text-to-image models towards a customizable product portfolio optimized for commercial deployment. Service providers gain flexibility to create an offering tailored to their customer base, introducing novel business models beyond simply vending the base model. This empowers profitably serving diverse market needs while monetizing their AI assets through product differentiation and pricing opportunities better matched to consumer segments. Extensive experiments validate our method’s ability to create purposeful model customizations across various domains and applications. Our contributions include:

- We introduce a novel task called “training-free editioning” for text-to-image models, which aims to create customized variations or editions of a base model without expensive retraining.
- We propose a novel method to achieve training-free editioning by formulating different model editions as *concept subspaces* within the text embedding space of the base model, leveraging Principal Component Analysis (PCA) to obtain low-dimensional subspaces capturing desired concepts.
- Extensive experiments across various domains demonstrate the effectiveness of our approach in creating purposeful model customizations suited for different user groups and applications. We highlight the business potential of training-free editioning in enabling service providers to offer differentiated product editions, innovative pricing strategies, and tailored solutions optimized for commercial deployment.

2 Related Work

Text-to-Image Synthesis. Driven by the success of deep generative models, text-to-image synthesis has become a rapidly evolving field in computer vision and machine learning that aims to generate realistic images from textual descriptions. One of the pioneering works in this field is

AlignDRAW [21], which introduced an attention-based approach that generates images by drawing a sequence of patches on the canvas based on an input caption. While this method represented a promising step forward, the generated images often lacked coherence and failed to accurately reflect the input textual descriptions. The advent of generative adversarial networks (GANs) ushered in a new era of text-to-image synthesis techniques. Text-conditional GANs [26] were among the first to leverage the adversarial training framework for this task. Subsequently, methods like StackGAN [39], AttnGAN [34], and ControlGAN [18] demonstrated improved performance by incorporating attention mechanisms and hierarchical architectures. Despite their notable achievements, these GAN-based approaches often struggled to maintain high consistency, resolution, and diversity in the generated images, falling short of meeting the demanding requirements of real-world applications. A significant breakthrough in text-to-image synthesis emerged with the introduction of large-scale datasets and transformer-based models. OpenAI’s DALL-E [25] pioneered the use of vast text-image pairs, enabling the generation of high-quality images from textual descriptions. Building upon this success, Parti [37] further demonstrated the potential of scaling up data and models for improved text-to-image generation performance. Nevertheless, thanks to their stable training and flexible conditioning (e.g., text, image, and other modalities), diffusion models [27] have dominated the state-of-the-art solutions for text-to-image synthesis.

Diffusion Models. Diffusion models are a class of deep generative models that have recently demonstrated remarkable performance in generating high-quality samples across various applications. These models are parameterized Markov chains trained using variational inference to generate samples that match the data distribution after a finite number of iterations [29, 12]. Diffusion implicit models [30], which are based on a class of non-Markovian diffusion processes, lead to the same training objective as traditional diffusion models, but can produce high-quality samples more efficiently. A representative framework for training diffusion models in the latent space is *Stable Diffusion*, a scaled-up version of the Latent Diffusion Model (LDM) [27]. Thanks to its flexibility allowing for multi-modal control signals (including text), Stable Diffusion has captivated the imagination of many users and dominated the field, especially in the open-source community. For example, [5] proposed a novel approach to create variations of a given “concept” by representing it with a single word embedding; Prompt-to-prompt [9] focuses on manipulating the attention maps corresponding to the text embeddings for editing images in pre-trained text-conditioned diffusion models; Null-text inversion [22] proposed performing DDIM inversion on the input image with related prompts into the latent space of a text-guided diffusion model, enabling intuitive text-based image editing. These efforts, while effective, have focused primarily on extending the technical power and usability of the text-to-image (diffusion) model, whose business model is still immature.

To bridge this gap, we propose a novel task called *training-free editioning* for text-to-image models, which aims to create customized variations or editions of a base model without expensive retraining. This enables service providers to offer differentiated product editions, innovative pricing strategies, and tailored solutions optimized for commercial deployment.

3 Task Definition

We define the **training-free editioning** task for text-to-image models as follows:

Definition 1 (General). Given a trained general-purpose text-to-image model M , let $C = \{c_1, c_2, \dots, c_n\}$ be a list of n concepts (textual) to be editioned on, p be an input prompt to M , we denote the image synthesized by M but editioned on C as:

$$I = M(p \mid C), \tag{1}$$

where I is restricted to only contain concepts in C .

Despite its generality, Definition 1 lacks specifications for both the concept list C and prompts p , posing challenges for both problem-solving and evaluation. As a first step in addressing this grand challenge, we propose a “Special” definition of the proposed task as follows:

Definition 2 (Special). Given a trained general-purpose text-to-image model M , let p_T be an input prompt to M following a template T with one of the most basic linguistic topologies:

$$T = \langle \text{subject} \rangle \langle \text{verb} \rangle \langle \text{preposition} \rangle \langle \text{object} \rangle, \tag{2}$$

and let $C = \{c_1, c_2, \dots, c_n\}$ be a list of concepts for all elements in p_T (e.g., “cat” for subject, “jumping” for verb, “grass” for object), we denote the corresponding image synthesized by M but

editioned on C as:

$$I = M(p_T | C) \quad (3)$$

where the subject/verb/object in I belongs to C .

In this work, we focus on solving the problem outlined in Definition 2, which is an important first step towards solving the grand challenge and encompasses a large number of real-world use cases.

3.1 Differences with Image Editing and Concept Erasing

Editioning vs. Editing. Task-wise, text-to-image editing [15, 27, 9, 2, 22, 31, 35, 4] works at the *aspect/image-level*, which typically refers to the process of modifying or manipulating specific aspects of an existing image based on a text prompt or instructions while leaving irrelevant aspects of it unchanged, e.g., inpainting, outpainting, or style transfer. In contrast, the proposed text-to-image editioning task works at the *model-level*, which aims to customize the behavior of the text-to-image model itself to cater to specific user needs or functionalities. Methodology-wise, since editing works at the *aspect/image-level*, its key challenge is to disentangle the target aspect of an image that needs to be edited from the rest, e.g., by manipulating the attention maps of a given image [33, 14, 19, 9, 22]. On the contrary, our editioning task is performed at the *model level*, so its main challenge lies in controlling the model’s behavior, e.g., by manipulating the model’s text/image embedding space.

Editioning vs. Concept Erasing. Task-wise, our editioning and concept erasing can be viewed as *complementary tasks*, where our editioning aims to retain concept(s) c from a model and concept erasing aims to remove c from the model. Methodology-wise, existing concept erasing methods [6, 17, 7, 20, 13, 36, 38, 16] primarily focus on fine-tuning model weights. In contrast, our approach does not involve any training and concentrates on manipulating the model’s text/image embedding space directly. The choice of such distinct methodologies stems from the observation that C typically constitutes a relatively small subset compared to the entire set of concepts learned by the model. Consequently, for concept erasing, removing C can be achieved through a minor perturbation of the model weights. However, for our editioning task, retaining C and dropping all other concepts would necessitate a significant modification, akin to retraining the entire model from scratch.

4 Method

Addressing the problem outlined in Definition 2, a straightforward idea is to modify p_T by replacing its elements with those in C , *i.e.*:

$$p_T | C = p_{T(C)} \quad (4)$$

where $T(C) = \langle \text{subject} \in C \rangle \langle \text{verb} \in C \rangle \langle \text{preposition} \in C \rangle \langle \text{object} \in C \rangle$. However, this approach either requires prior knowledge of the template or requires complex syntax analysis to locate the replacement, and is thus not generalizable. To address this issue, we propose a novel approach, namely **Concept Subspace Projection**, which shifts the focus from prompts p_T to their embeddings and achieves $M(p_T | C)$ by projecting the embedding vector of p_T to a concept subspace $S_{T(C)}$ defined by $T(C)$. Specifically, let \mathcal{E} be the text encoder of M and $M(\cdot) = \hat{M}(\mathcal{E}(\cdot))$, $S = \mathbb{R}^d$ be the text (image) embedding space of M , we have:

$$I = M(p_T | C) = \hat{M}(\mathcal{E}(p_T | C)) = \hat{M}(PR_{S_{T(C)}}(\mathcal{E}(p_T))) \quad (5)$$

where $PR_x(y)$ denotes the projection of y on x , $S_{T(C)} = \mathbb{R}^{d_{T(C)}} \subset S$ denotes the concept subspace specified by the template T and concepts C , $d_{T(C)} < d$. In this way, we create the **C-edition** of M as the concept space $S_{T(C)}$.

4.1 CLIP-based Concept Subspace Projection

Recognizing that CLIP [24] dominates the implementation of \mathcal{E} in state-of-the-art text-to-image models [40, 27, 25, 28, 23, 1, 8], we follow this common practice and develop our method in the CLIP embedding space. Thanks to CLIP’s use of **cosine similarity** for comparing text and image embeddings, we hypothesize that (please see Sec. 5.3 for an empirical justification):

Conjecture 1. For CLIP encoders, the text embeddings in concept subspaces $S_{T(C)}$ corresponding to different C are on a thin **hypersphere shell centered at the origin**.

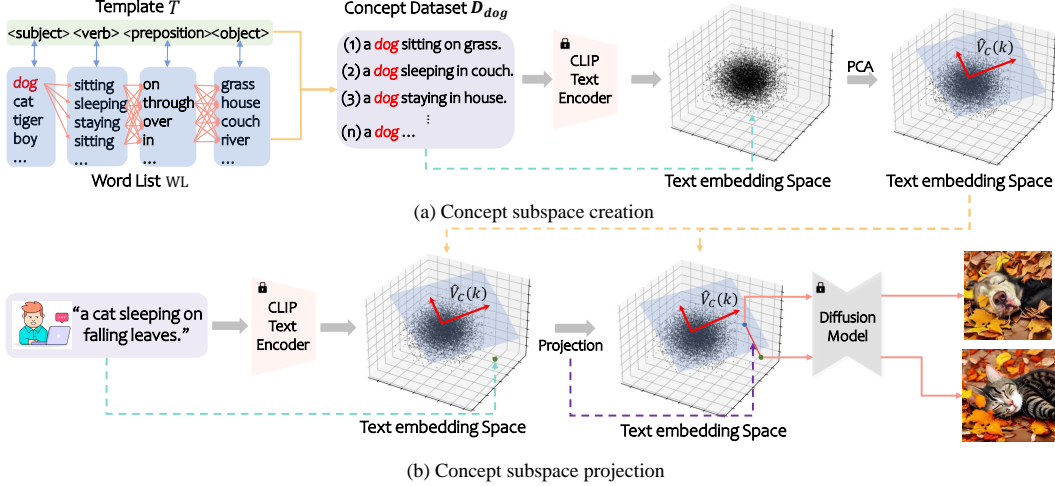


Figure 2: Overview of our concept subspace creation (top) and projection (bottom).

Concept Subspace Creation. Based on Conjecture 1, the concept subspace $S_{T(C)}$ accommodating the hypersphere shell can be characterized by a set of (orthogonal) vectors radiating from the origin. To obtain such vectors, we propose applying Principal Component Analysis (PCA) to a substantial sample of $\mathcal{E}(p_{T(C)})$ embeddings $D_C = [\mathcal{E}(p_{T(C)}^1), \mathcal{E}(p_{T(C)}^2), \dots, \mathcal{E}(p_{T(C)}^m)]$:

$$\mathbf{V}_C = \text{PCA}(D_C) \quad (6)$$

where \mathbf{V}_C denotes the principal axes ranked by descending principal values. Then, we define:

$$\hat{\mathbf{V}}_C(k) = \mathbf{V}_C[0 : k] \quad (7)$$

as the basis of subspace $S_{T(C)}$, where k is selected according to a 95% threshold of explained variance. Please see Sec. 5.4 for more details.

Magnitude-compensated Projection. With $\hat{\mathbf{V}}_c(k)$, we define the projection function PR as:

$$PR_{S_{T(C)}}(\mathcal{E}(p_T)) = \eta \cdot \hat{\mathbf{V}}_c(k) \cdot \hat{\mathbf{V}}_c(k)^T \cdot \mathcal{E}(p_T) \quad (8)$$

where $\eta = \frac{\|\mathcal{E}(p_T)\|}{\|\hat{\mathbf{V}}_c(k) \cdot \hat{\mathbf{V}}_c(k)^T \cdot \mathcal{E}(p_T)\|}$ is a parameter to compensate for the loss of magnitude during the projection. Note that we omit the centering step for simplicity, since the PCA subspace is also approximately centered at the origin (Conjecture 1).

Efficient Computation. Guided by the classic manifold hypothesis [3] that assumes the existence of low-dimensional representations of high-dimensional data, we apply PCA to a substantial random sample of CLIP text embeddings D_{all} to reduce the dimensionality of the original CLIP embedding space from $77 \times 768 = 59,136$ to 13,000. This “compression” significantly improves computational efficiency by roughly $(59,136/13,000)^2 \approx 20.7$ for the computation of covariance matrix in PCA (bottleneck), without sacrificing the performance (Fig. 3). Thus, unless specified otherwise, we employ the 13,000-dimensional reduced space as the CLIP text embedding space in our experiments.

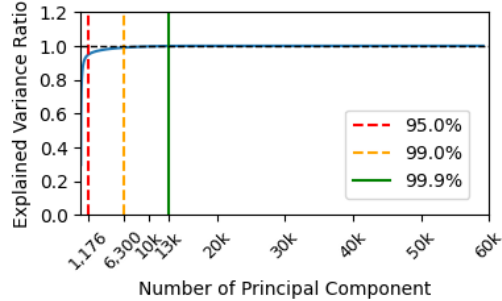


Figure 3: 13k components yield a cumulative explained variance ratio of 99.9+%.

5 Experiments

5.1 Experimental Setup

As mentioned above, our method consists of two steps: i) performing a low-loss dimensionality reduction to obtain an “efficient” CLIP embedding space of 13,000 dimensions; ii) creating concept

Table 1: CLIP score (softmax probability) of the images generated by our concept subspace projection, and their corresponding “ground truth” prompts (i.e., those accurately describing the image content).

Concept Subspace	Categories of Prompts in the Evaluation Datasets								
	Dog	Cat	Tiger	Car	Bus	Truck	Boy	Girl	Man
Dog Ed. (S_{dog})	\	0.9906±0.0550	0.9818±0.0830	0.9778±0.0959	0.9806±0.0899	0.9742±0.1075	0.9490±0.1172	0.9672±0.1054	0.9582±0.1539
Cat Ed. (S_{cat})	0.9938±0.0413	\	0.9302±0.1122	0.9786±0.1030	0.9859±0.0710	0.9783±0.1049	0.9463±0.1382	0.9632±0.1242	0.9624±0.1438
Tiger Ed. (S_{tiger})	0.9967±0.0356	0.9935±0.0278	\	0.9576±0.1633	0.9315±0.1869	0.8927±0.2465	0.9650±0.1487	0.9799±0.1018	0.9423±0.2051
Car Ed. (S_{car})	0.9580±0.1074	0.9435±0.1292	0.9445±0.1414	\	0.8950±0.2514	0.9551±0.1362	0.9210±0.1694	0.9145±0.1792	0.8740±0.2180
Bus Ed. (S_{bus})	0.8972±0.2474	0.9149±0.2206	0.9479±0.1676	0.9211±0.2243	\	0.9495±0.1728	0.9240±0.2232	0.8937±0.2603	0.8764±0.2894
Truck Ed. (S_{truck})	0.9471±0.1626	0.9265±0.1840	0.9764±0.0905	0.9155±0.2216	0.9830±0.0736	\	0.9573±0.1569	0.9121±0.2195	0.8997±0.2324
Boy Ed. (S_{boy})	0.9891±0.0526	0.9887±0.0652	0.9855±0.0569	0.9732±0.0963	0.9938±0.0448	0.9879±0.0606	\	0.9676±0.0919	0.9340±0.1320
Girl Ed. (S_{girl})	0.9920±0.0334	0.9907±0.0548	0.9905±0.0454	0.9612±0.1253	0.9884±0.0509	0.9804±0.0764	0.9261±0.1179	\	0.9536±0.1236
Man Ed. (S_{man})	0.9788±0.0665	0.9817±0.0659	0.9668±0.0861	0.9403±0.1545	0.9845±0.0677	0.9624±0.1134	0.8421±0.1923	0.9524±0.1411	\

Table 2: Evaluating the image synthesis capability of our concept space projection method using FID and IS scores. Ours: for each concept subspace, we take its evaluation dataset and generate their corresponding 8,000 images using the proposed concept space projection; SD: for each concept subspace, we replace the <object> of the prompts used in “Ours” with the concept of the subspace and generate 8,000 images using Stable Diffusion v1.4 [27]). SD’: different sets of 8,000 images generated in the same way as “SD”.

		Dog	Cat	Tiger	Car	Bus	Truck	Boy	Girl	Man	Mean
FID	Ours vs. SD	13.996	17.277	33.197	13.014	33.404	22.555	13.750	13.795	15.292	19.587
	SD vs. SD’	6.723	6.143	2.390	6.239	3.093	3.887	9.977	10.035	11.081	6.619
IS	Ours	10.081	3.964	2.678	5.693	4.030	3.774	9.361	9.421	11.125	6.680
	SD	8.551	2.531	1.155	4.357	2.209	1.940	8.707	8.897	10.507	5.428

spaces and projecting the embeddings of input prompts to them using the method proposed in Sec. 4. To implement them, we created the following datasets:

CLIP Dimensionality Reduction Dataset (D_{all}). CoCo 2017 Dataset [32] contains thousands of image and caption pairs, where each caption briefly describes the object, action, and subject of the image, e.g., “a cat laying on top of a counter looking down”. We randomly selected a subset of 160,000 captions from it and embedded them with CLIP to create the dataset D_{all} for the dimensionality reduction in creating the 13, 000-dimension “efficient” CLIP embedding space.

Concept Datasets. First, we construct a word list WL for each element of the template $T = \langle \text{subject} \rangle \langle \text{verb} \rangle \langle \text{preposition} \rangle \langle \text{object} \rangle$ (Eq. 2) and create a base dataset $D_{\text{all_concept}}$ containing all combinations of prompts created using T and WL . Without loss of generality, we focus on the different $\langle \text{subject} \rangle$ in our main experiments as they represent an important type of text-to-image model edition. Thus, we create the concept datasets for each $\langle \text{subject} \rangle$ by filter out all the prompts in $D_{\text{all_concept}}$ that do not contain the $\langle \text{subject} \rangle$ (e.g., D_{cat} , D_{dog}). Please see Appendix A for more details.

Concept Subspaces Creation and Evaluation. We follow the method detailed in Sec. 4.1 to create our concept subspaces (e.g., S_{cat} , S_{dog}) using their corresponding concept datasets (e.g., D_{cat} , D_{dog}), respectively. In addition, given a concept subspace $S_{\langle \text{subject} \rangle}$, we construct its evaluation dataset by sampling 1,000 random samples for each of the 8 categories in the complement set $\hat{D}_{\langle \text{subject} \rangle} = D_{\text{all_concept}} \setminus D_{\langle \text{subject} \rangle}$, totaling 8,000 samples.

Evaluation Metrics. We use i) the CLIP score [10] to measure the consistency between an image generated by our method and its corresponding descriptions (before and after our content subspace projection); ii) Frechet Inception Distance (FID) [11] and Inception Score (IS) to measure the image synthesis ability of the base model and its editions created by our method.

5.2 Effectiveness of Concept Subspace Projection for Text-to-Image Model Editioning

5.2.1 Quantitative Results

Editioning Accuracy. We use the CLIP score (probability) [10] to measure the editioning accuracy of our method, with 0 indicating low accuracy and 1 indicating high accuracy. Specifically, given a concept space S (e.g., cat edition S_{cat}) created using D (e.g., D_{cat}) defined in Sec. 5.1, for each input prompt \hat{p} in its corresponding evaluation dataset \hat{D} (e.g., \hat{D}_{cat} , all prompts without “cat”), we



Figure 4: Images generated by different prompts when using different editions of the Stable Diffusion v1.4 model. The input prompts are shown at the top.

compute the softmax probability of: i) the CLIP score between the images I generated using the projected prompts and their corresponding “ground truth” prompts p , i.e., the p in D that is equivalent to replacing the corresponding concept c in \hat{p} with that of D (e.g., “dog” to “cat” in p); ii) the CLIP score between I and p . Since the sum of the two probabilities is 1, we report the former in Table 1, which demonstrates that our concept subspace projection accurately restricts the generation to the concept of S (all scores are high).

Table 3: Cosine similarities between the input prompt, its projected version, and its “replaced” version. The “replaced” version refers to the text embedding of the prompt created by replacing the target component in the input prompt (e.g., “dog”) with that of the concept subspace (e.g., “cat”) being projected onto. The input prompts used are from the evaluation dataset of the corresponding subspace.

	$d(\text{input, replace})$	$d(\text{project, replace})$		$d(\text{input, replace})$	$d(\text{project, replace})$
Dog Ed. (S_{dog})	0.212 ± 0.050	0.059 ± 0.018	Truck Ed. (S_{truck})	0.250 ± 0.064	0.102 ± 0.031
Cat Ed. (S_{cat})	0.215 ± 0.058	0.067 ± 0.022	Boy Ed. (S_{boy})	0.206 ± 0.070	0.063 ± 0.022
Tiger Ed. (S_{tiger})	0.253 ± 0.063	0.085 ± 0.025	Girl Ed. (S_{girl})	0.221 ± 0.067	0.064 ± 0.024
Bus Ed. (S_{bus})	0.275 ± 0.062	0.108 ± 0.029	Man Ed. (S_{man})	0.198 ± 0.061	0.062 ± 0.021
Car Ed. (S_{car})	0.217 ± 0.052	0.076 ± 0.025	Mean	0.227	0.076

Image Synthesis Capability. We use the FID and IS scores to measure the image synthesis capability, with reference to those of the base model, i.e., Stable Diffusion (SD) v1.4 [27]. As Table 2 shows, the FID scores of our method are worse than those of SD but our IS scores are higher, indicating that our method generates similarly high quality but less diverse images than SD.

Similarity between Text Embeddings. To further characterize our content subspace projection, we compute the cosine similarities between the input prompt, its projected version, and its “replaced” version, where the “replaced” version refers to the text embedding of the prompt created by replacing the target component in the input prompt (e.g., “dog”) with that of the concept subspace (e.g., “cat”) being projected onto. As Table 3 shows, the projected embeddings are very close to the “replaced” ones, indicating that our projection is successful.

5.2.2 Qualitative Results

Editioning Accuracy. As Fig. 4 shows, we achieved a high editioning accuracy as the target concept (i.e., $\langle \text{subject} \rangle$) of the input prompt is restricted to the concept subspace while other concepts (i.e., $\langle \text{verb} \rangle$, $\langle \text{object} \rangle$) remain unchanged.

Image Synthesis Capability. As Fig. 5 shows, the images generated using our concept subspace projection are of similarly high quality and diversity to those generated by the base model directly.

5.3 Properties of CLIP Concept Subspaces

Distance to Origin. As Fig. 6 shows, we plot the histogram of the distances of text embeddings to the origin for each concept dataset and the Coco 2017 dataset. It can be observed that for all datasets, the distances are around 250 with small standard deviations, which justifies our Conjecture 1.

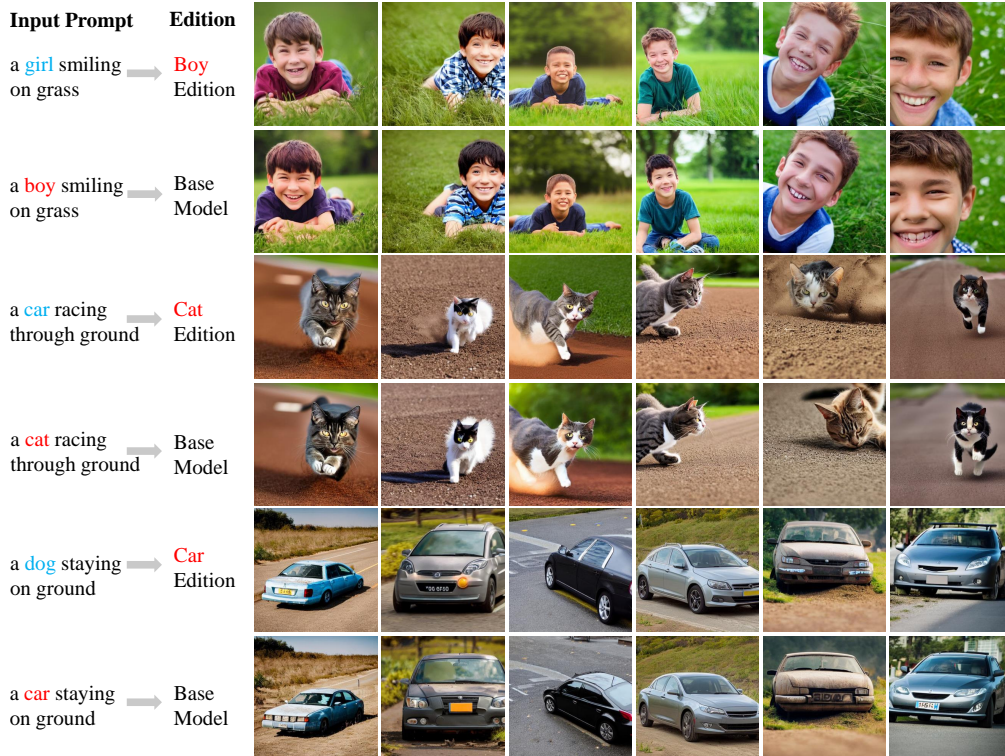


Figure 5: Different images generated by the same prompt when using different editions of the Stable Diffusion v1.4 model. The input prompts are shown at the bottom.

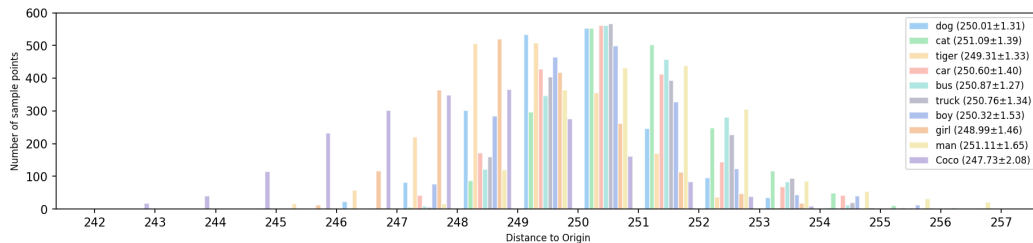


Figure 6: Distances of text embeddings to the origin. We randomly selected 2,000 prompts from each concept dataset and the Coco 2017 dataset to calculate the distances of samples to the origin. The mean and standard deviation values of the distances are shown in the legend.

Semantic Directions in Concept Subspace. As Fig. 7 shows, we observed that the principal components of each concept subspace also have semantic meanings. In addition, the content of the image remains restricted to its corresponding conceptual subspace (edition).

Concept Subspace Interpolation. As Fig. 8 shows, our concept subspace also allows for linear interpolation between projected text embeddings.

Table 4: Choice of k (Eq. 7) by 95% explained variance ratio for each concept subspace.

	Dog	Cat	Tiger	Car	Bus	Truck	Boy	Girl	Man
# of Principal Components	30	29	27	29	30	30	33	33	34

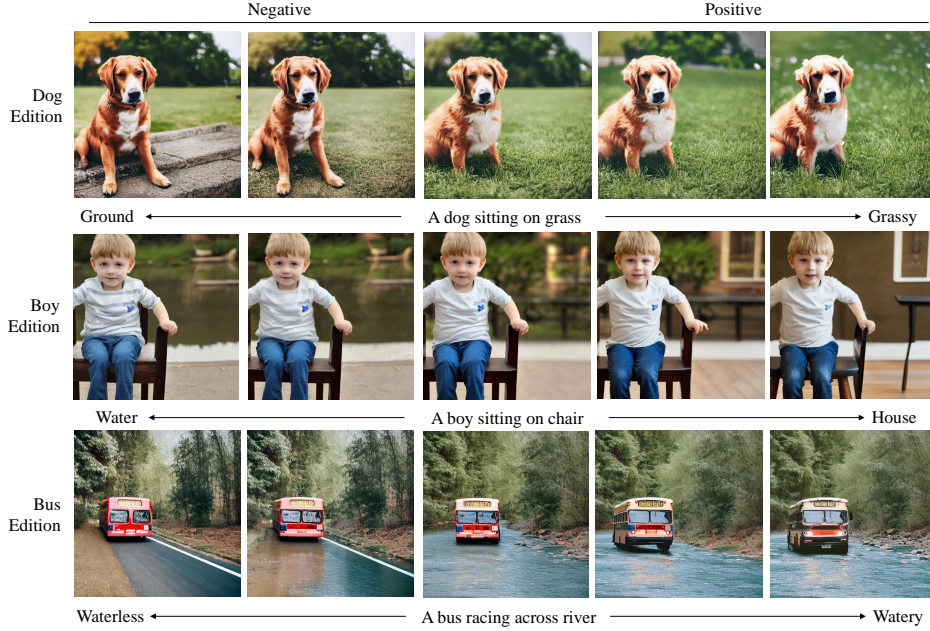


Figure 7: Images generated by moving text embeddings (the input prompt is shown in the middle) along the directions of principal components (PC). Row 1: PC #7; Row 2: PC #14; Row 3: PC #0.

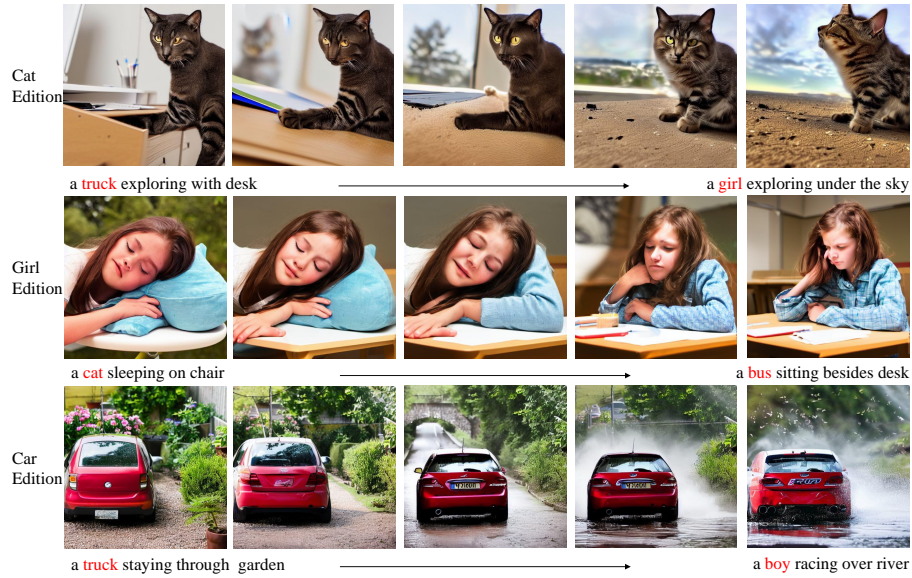


Figure 8: Linear interpolation between projected text embeddings. The input prompts are shown at the bottom. The words in red denote the <subject> to be restricted to the edition given on the left.

5.4 Choice of k for Each Concept Subspace

As Table 4 shows, empirically, we choose k (Eq. 7) for each concept subspace by the threshold of 95% explained variance ratio of that subspace.

6 Conclusion

Inspired by software editing, we propose training-free “editing” of text-to-image models by identifying *concept subspaces* within the latent space of their text encoders (e.g., CLIP). These

subspaces, obtained via applying Principal Component Analysis (PCA) on representative text embeddings, correspond to specific domains or attributes like “generating images of a cat lying on the grass/ground/falling leaves”. Projecting the text embedding of a given prompt into these low-dimensional subspaces enables efficient model customization without retraining. This unlocks novel business models, such as offering restricted “cat editions” that only generate cat images regardless of objects in input prompts, enabling new product differentiation and pricing strategies.

References

- [1] James Betker, Gabriel Goh, Li Jing, Tim Brooks, Jianfeng Wang, Linjie Li, Long Ouyang, Juntang Zhuang, Joyce Lee, Yufei Guo, et al. Improving image generation with better captions. *Computer Science*. <https://cdn.openai.com/papers/dall-e-3.pdf>, 2(3):8, 2023.
- [2] Tim Brooks, Aleksander Holynski, and Alexei A Efros. Instructpix2pix: Learning to follow image editing instructions. In *Proceedings of the IEEE/CVF Conference on Computer Vision and Pattern Recognition*, pages 18392–18402, 2023.
- [3] Bradley CA Brown, Anthony L Caterini, Brendan Leigh Ross, Jesse C Cresswell, and Gabriel Loaiza-Ganem. Verifying the union of manifolds hypothesis for image data. In *The Eleventh International Conference on Learning Representations*, 2022.
- [4] Guillaume Couairon, Jakob Verbeek, Holger Schwenk, and Matthieu Cord. Diffedit: Diffusion-based semantic image editing with mask guidance. *arXiv preprint arXiv:2210.11427*, 2022.
- [5] Rinon Gal, Yuval Alaluf, Yuval Atzmon, Or Patashnik, Amit H. Bermano, Gal Chechik, and Daniel Cohen-Or. An image is worth one word: Personalizing text-to-image generation using textual inversion, 2022.
- [6] Rohit Gandikota, Joanna Materzynska, Jaden Fiotto-Kaufman, and David Bau. Erasing concepts from diffusion models. *arXiv preprint arXiv:2303.07345*, 2023.
- [7] Rohit Gandikota, Hadas Orgad, Yonatan Belinkov, Joanna Materzyńska, and David Bau. Unified concept editing in diffusion models. In *Proceedings of the IEEE/CVF Winter Conference on Applications of Computer Vision*, pages 5111–5120, 2024.
- [8] Shuyang Gu, Dong Chen, Jianmin Bao, Fang Wen, Bo Zhang, Dongdong Chen, Lu Yuan, and Baining Guo. Vector quantized diffusion model for text-to-image synthesis. In *Proceedings of the IEEE/CVF Conference on Computer Vision and Pattern Recognition*, pages 10696–10706, 2022.
- [9] Amir Hertz, Ron Mokady, Jay Tenenbaum, Kfir Aberman, Yael Pritch, and Daniel Cohen-Or. Prompt-to-prompt image editing with cross attention control. 2022.
- [10] Jack Hessel, Ari Holtzman, Maxwell Forbes, Ronan Le Bras, and Yejin Choi. Clipscore: A reference-free evaluation metric for image captioning. *arXiv preprint arXiv:2104.08718*, 2021.
- [11] Martin Heusel, Hubert Ramsauer, Thomas Unterthiner, Bernhard Nessler, and Sepp Hochreiter. Gans trained by a two time-scale update rule converge to a local nash equilibrium. *Advances in neural information processing systems*, 30, 2017.
- [12] Jonathan Ho, Ajay Jain, and Pieter Abbeel. Denoising diffusion probabilistic models. *Advances in neural information processing systems*, 33:6840–6851, 2020.
- [13] Chi-Pin Huang, Kai-Po Chang, Chung-Ting Tsai, Yung-Hsuan Lai, and Yu-Chiang Frank Wang. Receler: Reliable concept erasing of text-to-image diffusion models via lightweight erasers. *arXiv preprint arXiv:2311.17717*, 2023.
- [14] Xuan Ju, Ailing Zeng, Yuxuan Bian, Shaoteng Liu, and Qiang Xu. Direct inversion: Boosting diffusion-based editing with 3 lines of code. *arXiv preprint arXiv:2310.01506*, 2023.
- [15] Bahjat Kawar, Shiran Zada, Oran Lang, Omer Tov, Huiwen Chang, Tali Dekel, Inbar Mosseri, and Michal Irani. Imagic: Text-based real image editing with diffusion models. In *Proceedings of the IEEE/CVF Conference on Computer Vision and Pattern Recognition*, pages 6007–6017, 2023.
- [16] Sanghyun Kim, Seohyeon Jung, Balhae Kim, Moonseok Choi, Jinwoo Shin, and Juho Lee. Towards safe self-distillation of internet-scale text-to-image diffusion models. *arXiv preprint arXiv:2307.05977*, 2023.

- [17] Nupur Kumari, Bingliang Zhang, Sheng-Yu Wang, Eli Shechtman, Richard Zhang, and Jun-Yan Zhu. Ablating concepts in text-to-image diffusion models. In *Proceedings of the IEEE/CVF International Conference on Computer Vision*, pages 22691–22702, 2023.
- [18] Bowen Li, Xiaojuan Qi, Thomas Lukasiewicz, and Philip Torr. Controllable text-to-image generation. *Advances in Neural Information Processing Systems*, 32, 2019.
- [19] Senmao Li, Joost van de Weijer, Taihang Hu, Fahad Shahbaz Khan, Qibin Hou, Yaxing Wang, and Jian Yang. Stylediffusion: Prompt-embedding inversion for text-based editing. *arXiv preprint arXiv:2303.15649*, 2023.
- [20] Zhili Liu, Kai Chen, Yifan Zhang, Jianhua Han, Lanqing Hong, Hang Xu, Zhenguo Li, Dit-Yan Yeung, and James Kwok. Geom-erasing: Geometry-driven removal of implicit concept in diffusion models. *arXiv preprint arXiv:2310.05873*, 2023.
- [21] Elman Mansimov, Emilio Parisotto, Jimmy Lei Ba, and Ruslan Salakhutdinov. Generating images from captions with attention. *arXiv preprint arXiv:1511.02793*, 2015.
- [22] Ron Mokady, Amir Hertz, Kfir Aberman, Yael Pritch, and Daniel Cohen-Or. Null-text inversion for editing real images using guided diffusion models. In *Proceedings of the IEEE/CVF Conference on Computer Vision and Pattern Recognition (CVPR)*, pages 6038–6047, June 2023.
- [23] Alex Nichol, Prafulla Dhariwal, Aditya Ramesh, Pranav Shyam, Pamela Mishkin, Bob McGrew, Ilya Sutskever, and Mark Chen. Glide: Towards photorealistic image generation and editing with text-guided diffusion models. *arXiv preprint arXiv:2112.10741*, 2021.
- [24] Alec Radford, Jong Wook Kim, Chris Hallacy, Aditya Ramesh, Gabriel Goh, Sandhini Agarwal, Girish Sastry, Amanda Askell, Pamela Mishkin, Jack Clark, et al. Learning transferable visual models from natural language supervision. In *International conference on machine learning*, pages 8748–8763. PMLR, 2021.
- [25] Aditya Ramesh, Mikhail Pavlov, Gabriel Goh, Scott Gray, Chelsea Voss, Alec Radford, Mark Chen, and Ilya Sutskever. Zero-shot text-to-image generation. In *International Conference on Machine Learning*, pages 8821–8831. PMLR, 2021.
- [26] Scott Reed, Zeynep Akata, Xinchun Yan, Lajanugen Logeswaran, Bernt Schiele, and Honglak Lee. Generative adversarial text to image synthesis. In *International conference on machine learning*, pages 1060–1069. PMLR, 2016.
- [27] Robin Rombach, Andreas Blattmann, Dominik Lorenz, Patrick Esser, and Björn Ommer. High-resolution image synthesis with latent diffusion models. In *Proceedings of the IEEE/CVF conference on computer vision and pattern recognition*, pages 10684–10695, 2022.
- [28] Chitwan Saharia, William Chan, Saurabh Saxena, Lala Li, Jay Whang, Emily L Denton, Kamyar Ghasemipour, Raphael Gontijo Lopes, Burcu Karagol Ayan, Tim Salimans, et al. Photorealistic text-to-image diffusion models with deep language understanding. *Advances in Neural Information Processing Systems*, 35:36479–36494, 2022.
- [29] Jascha Sohl-Dickstein, Eric Weiss, Niru Maheswaranathan, and Surya Ganguli. Deep unsupervised learning using nonequilibrium thermodynamics. In *International conference on machine learning*, pages 2256–2265. PMLR, 2015.
- [30] Jiaming Song, Chenlin Meng, and Stefano Ermon. Denoising diffusion implicit models. *arXiv preprint arXiv:2010.02502*, 2020.
- [31] Narek Tumanyan, Michal Geyer, Shai Bagon, and Tali Dekel. Plug-and-play diffusion features for text-driven image-to-image translation. In *Proceedings of the IEEE/CVF Conference on Computer Vision and Pattern Recognition*, pages 1921–1930, 2023.
- [32] 2014 TY Lin. Coco 2017.
- [33] Sihan Xu, Yidong Huang, Jiayi Pan, Ziqiao Ma, and Joyce Chai. Inversion-free image editing with natural language. *arXiv preprint arXiv:2312.04965*, 2023.
- [34] Tao Xu, Pengchuan Zhang, Qiuyuan Huang, Han Zhang, Zhe Gan, Xiaolei Huang, and Xiaodong He. Attngan: Fine-grained text to image generation with attentional generative adversarial networks. In *Proceedings of the IEEE conference on computer vision and pattern recognition*, pages 1316–1324, 2018.

- [35] Binxin Yang, Shuyang Gu, Bo Zhang, Ting Zhang, Xuejin Chen, Xiaoyan Sun, Dong Chen, and Fang Wen. Paint by example: Exemplar-based image editing with diffusion models. In *Proceedings of the IEEE/CVF Conference on Computer Vision and Pattern Recognition*, pages 18381–18391, 2023.
- [36] Ahmet Burak Yildirim, Vedat Baday, Erkut Erdem, Aykut Erdem, and Aysegul Dundar. Inst-inpaint: Instructing to remove objects with diffusion models. *arXiv preprint arXiv:2304.03246*, 2023.
- [37] Jiahui Yu, Yuanzhong Xu, Jing Yu Koh, Thang Luong, Gunjan Baid, Zirui Wang, Vijay Vasudevan, Alexander Ku, Yinfei Yang, Burcu Karagol Ayan, et al. Scaling autoregressive models for content-rich text-to-image generation. *arXiv preprint arXiv:2206.10789*, 2(3):5, 2022.
- [38] Eric Zhang, Kai Wang, Xingqian Xu, Zhangyang Wang, and Humphrey Shi. Forget-me-not: Learning to forget in text-to-image diffusion models. *arXiv preprint arXiv:2303.17591*, 2023.
- [39] Han Zhang, Tao Xu, Hongsheng Li, Shaoting Zhang, Xiaogang Wang, Xiaolei Huang, and Dimitris N Metaxas. Stackgan: Text to photo-realistic image synthesis with stacked generative adversarial networks. In *Proceedings of the IEEE international conference on computer vision*, pages 5907–5915, 2017.
- [40] Lvmin Zhang, Anyi Rao, and Maneesh Agrawala. Adding conditional control to text-to-image diffusion models. In *Proceedings of the IEEE/CVF International Conference on Computer Vision*, pages 3836–3847, 2023.

A Details of Concept Datasets

As Table 5 shows, we construct a word list WL for each element of the template $T = \langle \text{subject} \rangle \langle \text{verb} \rangle \langle \text{preposition} \rangle \langle \text{object} \rangle$ (Eq. 2) and create a base dataset $D_{\text{all_concept}}$ containing all combinations of prompts created using T and WL , resulting in a total of $9 \times 21 \times 8 \times 21 = 31,752$ prompts. Without loss of generality, we focus on the different $\langle \text{subject} \rangle$ in our main experiments as they represent an important type of text-to-image model edition. Thus, we create the concept datasets for each $\langle \text{subject} \rangle$ by filtering out all the prompts in $D_{\text{all_concept}}$ that do not contain the $\langle \text{subject} \rangle$ (e.g., D_{cat} , D_{dog}), resulting in $21 \times 8 \times 21 = 3,528$ prompts per subspace.

Table 5: Word list for each element of the template $T = \langle \text{subject} \rangle \langle \text{verb} \rangle \langle \text{preposition} \rangle \langle \text{object} \rangle$ (Eq. 2).

subject	verb	preposition	object
cat	sleeping	on	ground
tiger	exploring	with	sky
dog	moving	in	river
car	lounging	over	bed
bus	lying	through	chair
truck	gazing	out	desk
boy	chasing	besides	grass
girl	stretching	under	seat
man	standing		couch
	stalking		backyard
	leaping		garden
	talking		house
	running		leaves
	jumping		road
	napping		station
	staying		path
	sitting		stop
	smiling		street
	racing		yard
	stopping		field
	waiting		way

B Results on Stable Diffusion v1.5

As shown in Table 6 and Fig. 9, our method also generalizes to Stable Diffusion v1.5 and achieves similarly high CLIP scores and editioning accuracy.

Table 6: CLIP score (softmax probability) of the images generated by our concept subspace projection, and their corresponding “ground truth” prompts (i.e., those accurately describing the image content).

Concept Subspace	Categories of Prompts in the Evaluation Datasets								
	Dog	Cat	Tiger	Car	Bus	Truck	Boy	Girl	Man
Dog Ed. (S_{dog})	\	0.9923±0.0523	0.9864±0.0804	0.9778±0.1054	0.9852±0.0750	0.9634±0.1451	0.9605±0.0956	0.9739±0.1004	0.9816±0.0762
Cat Ed. (S_{cat})	0.9891±0.0694	\	0.9370±0.1177	0.9781±0.1102	0.9813±0.0878	0.9600±0.1525	0.9540±0.1292	0.9609±0.1460	0.9557±0.1719
Tiger Ed. (S_{tiger})	0.9907±0.0645	0.9928±0.0293	\	0.9438±0.1837	0.9562±0.1450	0.9262±0.1990	0.9675±0.1471	0.9815±0.0945	0.9352±0.2149
Car Ed. (S_{car})	0.9714±0.0853	0.9571±0.1075	0.9711±0.0747	\	0.9605±0.1437	0.9741±0.0813	0.9558±0.1119	0.9322±0.1540	0.8941±0.1876
Bus Ed. (S_{bus})	0.9748±0.1147	0.9813±0.0873	0.9895±0.0571	0.9565±0.1628	\	0.9806±0.0989	0.9897±0.0768	0.9737±0.1312	0.9701±0.1397
Truck Ed. (S_{truck})	0.9883±0.0660	0.9743±0.1046	0.9862±0.0852	0.9666±0.1227	0.9962±0.0202	\	0.9896±0.0498	0.9863±0.0788	0.9759±0.0692
Boy Ed. (S_{boy})	0.9932±0.0322	0.9924±0.0450	0.9916±0.0499	0.9684±0.1272	0.9923±0.0563	0.9821±0.0852	\	0.9730±0.0836	0.9571±0.1059
Girl Ed. (S_{girl})	0.9900±0.0530	0.9934±0.0243	0.9919±0.0465	0.9686±0.1093	0.9874±0.0643	0.9824±0.0781	0.9330±0.1145	\	0.9688±0.0974
Man Ed. (S_{man})	0.9796±0.0777	0.9890±0.0395	0.9806±0.0647	0.9334±0.1783	0.9911±0.0390	0.9668±0.1040	0.8698±0.1644	0.9700±0.0922	\

C Concept Subspaces of $\langle \text{verb} \rangle$ and $\langle \text{object} \rangle$

Following a similar experimental setup used for $\langle \text{subject} \rangle$ in the main paper, we show that the proposed method can also be applied to $\langle \text{verb} \rangle$ and $\langle \text{object} \rangle$ of the template $T = \langle \text{subject} \rangle \langle \text{verb} \rangle \langle \text{preposition} \rangle \langle \text{object} \rangle$ (Eq. 2). As shown in Table 7, Fig. 10, Fig. 11, our method can also accurately restrict the generation to the concept subspace.

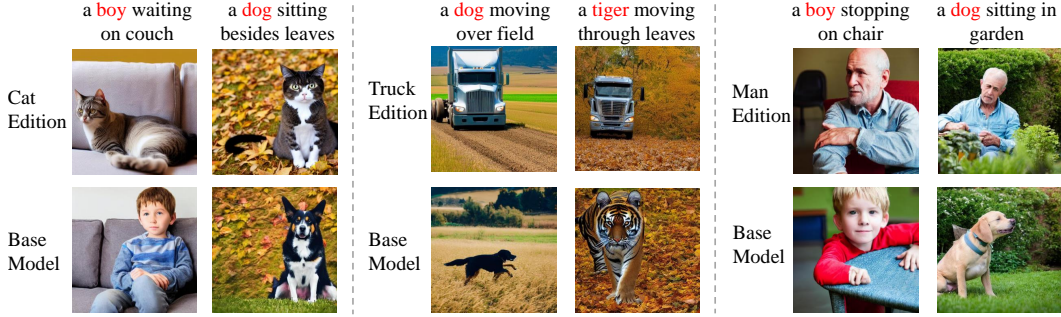


Figure 9: Images generated by different prompts when using different editions of the Stable Diffusion v1.5 model. The input prompts are shown at the top.

Table 7: CLIP score (softmax probability) of the images generated by our concept subspace projection, and their corresponding “ground truth” prompts (i.e., those accurately describing the image content) for (a) $\langle \text{verb} \rangle$ and (b) $\langle \text{object} \rangle$ of the template $T = \langle \text{subject} \rangle \langle \text{verb} \rangle \langle \text{preposition} \rangle \langle \text{object} \rangle$ (Eq. 2)

(a)

Concept Subspace	Verb		
	Sitting	Sleeping	Racing
Sitting Ed. (S_{sitting})	—	0.8085 ± 0.2048	0.8060 ± 0.2373
Sleeping Ed. (S_{sleeping})	0.8011 ± 0.2544	—	0.8051 ± 0.2743
Racing Ed. (S_{racing})	0.8167 ± 0.2685	0.9001 ± 0.1980	—

(b)

Concept Subspace	Object		
	Grass	Leaves	Desk
Grass Ed. (S_{grass})	—	0.8986 ± 0.1566	0.9223 ± 0.1640
Leaves Ed. (S_{leaves})	0.7488 ± 0.3467	—	0.7431 ± 0.3253
Desk Ed. (S_{desk})	0.7151 ± 0.3393	0.6771 ± 0.3329	—



Figure 10: Concept Subspaces of $\langle \text{verb} \rangle$. Images generated by different prompts when using different editions of the Stable Diffusion v1.4 model. The input prompts are shown at the top. The left clarifies the different editions of the object and the base model.

D Effectiveness of Our Magnitude-compensated Projection

Distances of Text Embeddings to the Origin after Naive Projection. To demonstrate the necessity of our magnitude-compensated projection (Eq. 8), we show that the distances indeed reduce after naive projections (Fig. 12).



Figure 11: Concept Subspaces of $\langle \text{object} \rangle$. Images generated by different prompts when using different editions of the Stable Diffusion v1.4 model. The input prompts are shown at the top. The left clarifies the different editions of the object and the base model.

Qualitative Comparison. As Fig. 13 shows, without our magnitude-compensated projection (i.e., naive projection), the generated images suffer from severe distortions, which further demonstrates the effectiveness of our magnitude-compensated projection.

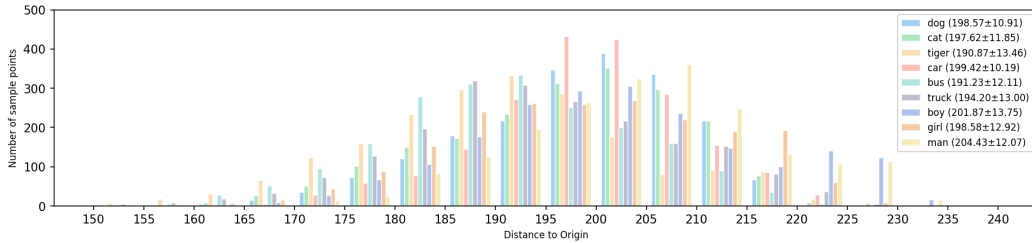


Figure 12: Distances of text embeddings to the origin after naive projection. We randomly selected 2,000 prompts from the evaluation dataset of a given concept space S and naively projected them to S . The mean and standard deviation values of the distances are shown in the legend.

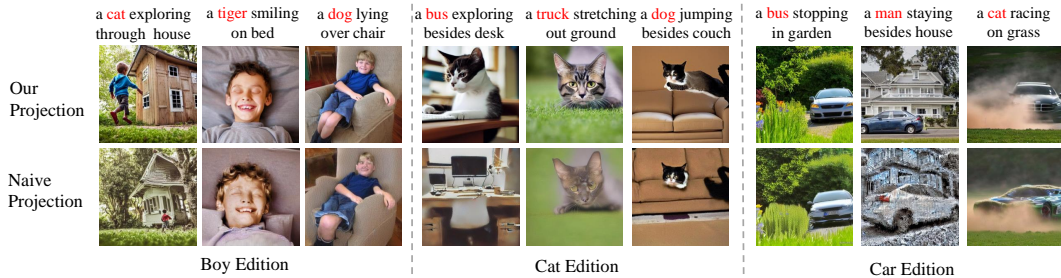


Figure 13: Comparison of images generated using naive projection and our magnitude-compensated projection. All images are generated with editions of the Stable Diffusion v1.4 model. The input prompts are shown at the top. The editions are shown at the bottom.

E Limitations

Our work is a first step toward the new task of “Training-free Editing of Text-to-image Models”. As such, it is constrained by the templates used, a limited list of words, and other factors. Nonetheless, we believe that our approach is a solid step forward and will inspire the community for subsequent innovations.

F Computational Resources

All experiments in our work are conducted on a workstation with an 12th-gen Intel Core i7-12700 CPU, an Nvidia RTX 4090 24G GPU, 64GB memory and a 1TB hard disk.